

# Incorporation of Silver Ions into Ultrathin Titanium Phosphate Films: In Situ Reduction to Prepare Silver Nanoparticles and Their Antibacterial Activity

Qifeng Wang, Huijun Yu, Ling Zhong, Junqiu Liu, Junqi Sun,\* and Jiacong Shen

Key Lab of Supramolecular Structure and Materials, College of Chemistry, Jilin University, Changchun, P. R. China 130012

Received December 1, 2005. Revised Manuscript Received February 3, 2006

Silver ions were incorporated into titanium phosphate ultrathin films by an ion-exchange process conducted at 50 °C and room temperature. The silver ions were dispersed homogeneously along the normal direction of titanium phosphate film, as confirmed by UV–vis spectroscopy and X-ray photoelectron spectroscopy. In situ reduction by NaBH<sub>4</sub> produced silver nanoparticles embedded in titanium phosphate film. The particle size is dependent on the ion-exchange temperature, where a higher temperature leads to a larger particle size. The silver-ion-exchanged titanium phosphate films are effective in prohibiting the growth of *Escherichia coli* and, therefore, are expected to be used as antibacterial coatings.

## Introduction

The incorporation of metal ions into solid films in a controlled way is very important for academic research and industrial applications.<sup>1</sup> On one hand, metal-ion-doped solid films can acquire new functions as compared to the undoped ones; on the other hand, in situ reactions can produce metal/semiconductor nanoparticles embedded in solid films, which can facilitate the application of the nanoparticles or combine the properties of the nanoparticles and the matrix films to produce novel properties that are beyond those of the individual components.<sup>2–5</sup> In this area, the incorporation of silver ions into various kinds of films is of great importance because of their wide range of applications in areas such as catalysis, optics, and hygiene, among others.<sup>6–11</sup> Multilayered polyelectrolyte films of polyethyleneimine (PEI)/poly(acrylic acid) (PAA) containing Ag nanoparticles can catalyze the electrochemical reduction of methylene bromide.<sup>6</sup> By selective incorporation of silver ions along the film normal direction into layer-by-layer-assembled polyelectrolyte multilayer films and in situ reduction, one-dimensional photonic structures that are uniform over a large area can be prepared, which provides a promising method for preparing integrated

optical circuits and optical sensors.<sup>7</sup> By photoelectrochemical reduction of Ag<sup>+</sup> to Ag nanoparticles in nanoporous TiO<sub>2</sub> films under UV light, Ag–TiO<sub>2</sub> films exhibiting multicolor photochromism have been obtained.<sup>8</sup> Silver ions have long been known to have strong inhibitory and bactericidal effects, as well as a broad spectrum of antimicrobial activities.<sup>12</sup> Polyelectrolyte multilayer films<sup>6,9,10</sup> and porous polymer microspheres<sup>11</sup> containing Ag nanoparticles show excellent antibacterial performance toward bacteria such as *Escherichia coli* (*E. coli*) and *Staphylococcus epidermidis* (*S. aureus*).

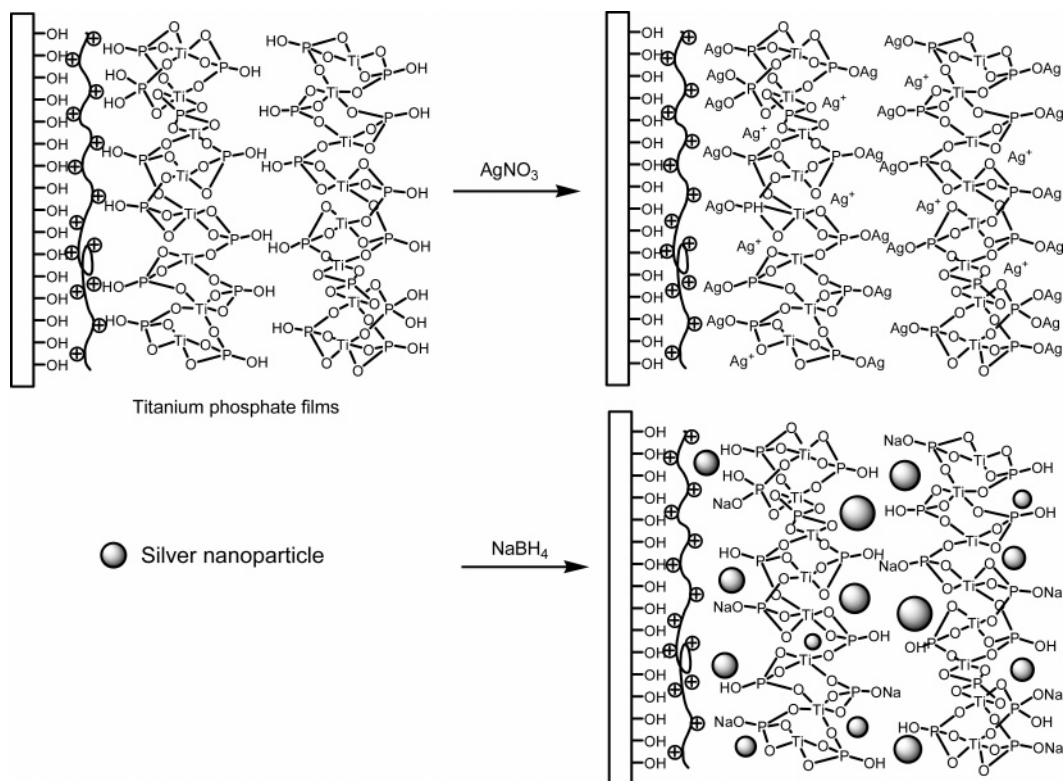
There are several methods for incorporating metal ions into solid films, depending on the preparative process of the matrix films. Silver ions can be incorporated into polyelectrolyte multilayer films either by immersion of a polyelectrolyte film containing ion-binding groups (such as carboxylic acid) into silver ion solution<sup>13</sup> or by layer-by-layer assembly of a polyelectrolyte–metal ion complex<sup>6</sup> with another complementary polyelectrolyte partner. Subsequent in situ reaction can produce Ag nanoparticles embedded in the ultrathin films. A composite Mg<sup>2+</sup>-doped TiO<sub>2</sub> film can be prepared by the surface sol–gel process from a mixture of matrix-forming titanium alkoxide and a magnesium alkoxide template. The subsequent removal of Mg<sup>2+</sup> ions by acid/base treatment creates ion-exchange sites in the TiO<sub>2</sub> matrix film that allows for the incorporation of a variety of metal ions, including silver ions.<sup>14</sup> Solid films prepared by sol–gel, dip-coating, and spin-coating techniques can be doped with metal ions during the film preparation process or during posttreatment by means of ion implantation, ion exchange, sputtering, etc.<sup>15–18</sup> The above-mentioned methods are widely

\* To whom correspondence should be addressed. Fax: 0086-431-5193421. E-mail: sun\_junqi@jlu.edu.cn.

- (1) Schmid, G. *Chem. Rev.* **1992**, *92*, 1709.
- (2) Ohno, T.; Haga, D.; Fujihara, K.; Kaizaki, K.; Matsumura, M. *J. Phys. Chem. B* **1997**, *101*, 6415.
- (3) Matsumoto, Y.; Kurimoto, J.; Shimizu, T.; Sato, E. *J. Electrochem. Soc.* **1981**, *128*, 1040.
- (4) Tanaka, T.; Takenaka, S.; Funabiki, T.; Yoshida, S. *J. Chem. Soc., Faraday Trans.* **1996**, *92*, 1975.
- (5) Takahara, Y.; Kondo, J. N.; Takata, T.; Lu, D.; Domen, K. *Chem. Mater.* **2001**, *13*, 1194.
- (6) Dai, J.; Bruening, M. L. *Nano Lett.* **2002**, *2*, 497.
- (7) Wang, T. C.; Cohen, R. E.; Rubner, M. F. *Adv. Mater.* **2002**, *14*, 1534.
- (8) Naoi, K.; Ohko, Y.; Tatsuma, T. *J. Am. Chem. Soc.* **2004**, *126*, 3664.
- (9) Lee, D.; Cohen, R. E.; Rubner, M. F. *Langmuir* **2005**, *21*, 9651.
- (10) Grunlan, J. C.; Choi, J. K.; Lin, A. *Biomacromolecules* **2005**, *6*, 1149.
- (11) Kim, J. W.; Lee, J. E.; Kim, S. J.; Lee, J. S.; Ryu, J. H.; Kim, J.; Han, S. H.; Chang, I. S.; Suh, K. D. *Polymer* **2004**, *45*, 4741.

- (12) Berger, T. J.; Spadaro, J. A.; Chapin, S. E.; Becker, R. O. *Antimicrob. Agents* **1996**, *357*.
- (13) Joly, S.; Kane, R.; Radzilowski, L.; Wang, T.; Wu, A.; Cohen, R. E.; Thomas, E. L.; Rubner, M. F. *Langmuir* **2000**, *16*, 1354.
- (14) He, J. H.; Ichinose, I.; Fujikawa, S.; Kunitake, T.; Nakao, A. *Chem. Mater.* **2002**, *14*, 3493.
- (15) Yazawa, T.; Kadono, K.; Tanaka, H.; Sakaguchi, T.; Tsubota, S.; Kuraoka, K.; Miya, M. *J. Non-Cryst. Solids* **1994**, *170*, 105.

Scheme 1. Ion Exchange and Nanoparticle Formation in Titanium Phosphate Ultrathin Films



applicable, but problems such as their complexity in preparation and narrow application window are shortcomings that require further improvements. For instance, although polyelectrolyte multilayers as matrix films are easily fabricated on substrates of any type and shape, they cannot generally endure harsh conditions such as high temperature, irradiation, scratching, and erosive solvents. Film preparation by dip-coating and spin-coating cannot be accomplished on surfaces with complicated morphologies.

Recently, we developed a facile layer-by-layer adsorption and reaction method for the preparation of titanium phosphate ultrathin films.<sup>19</sup> By repetitive adsorption of hydrated titanium from aqueous  $\text{Ti}(\text{SO}_4)_2$  solution and subsequent reaction with phosphate groups, ultrathin films of titanium phosphate can be easily fabricated. This method is characterized by its simplicity in film preparation and its ease in controlling film thickness and surface morphology. Titanium phosphate materials are chemically stable and have excellent ion-exchange properties.<sup>20,21</sup> It has been reported that silver-phosphate complex materials have a strong antibacterial ability.<sup>22</sup> When compared to zeolite-based silver materials, silver-phosphate complex materials show improved stability and no harmful effects upon contact with human skin.<sup>22</sup> In

this work, we showed that the incorporation of silver ions into titanium phosphate films can be easily achieved by a simple ion-exchange process. Subsequent in situ reduction can prepare silver nanoparticles embedded in the titanium phosphate films. The  $\text{Ag}^+$ -exchanged titanium phosphate films are effective in inhibiting bacteria growth. The chemical and mechanical stabilities of the matrix titanium phosphate films are expected to guarantee such films a wide application window in catalysis and hygiene.

## Experimental Section

**Materials.** Titanium sulfate [ $\text{Ti}(\text{SO}_4)_2$ ], sodium hydrogen phosphate ( $\text{Na}_2\text{HPO}_4 \cdot 12\text{H}_2\text{O}$ ), sodium dihydrogen phosphate ( $\text{NaH}_2\text{PO}_4 \cdot 2\text{H}_2\text{O}$ ), silver nitrate ( $\text{AgNO}_3$ ), and sodium borohydride ( $\text{NaBH}_4$ ) were of analytical grade and were purchased from Beijing Chemical Reagents Company. Poly(diallyldimethylammonium chloride) (PDDA) aqueous solution with a molecular weight of 100 000–200 000 was purchased from Sigma-Aldrich. Deionized water was used in all experiments. The phosphate salt (PS) solution comprised 0.1 M phosphate ( $\text{Na}_2\text{HPO}_4$  and  $\text{NaH}_2\text{PO}_4$ ) with its pH adjusted by the addition of  $\text{H}_2\text{SO}_4$ .

**Preparation of Titanium Phosphate Films.** Quartz and silicon wafers were immersed in slightly boiled piranha solution (3:1 mixture of 98%  $\text{H}_2\text{SO}_4$  and 30%  $\text{H}_2\text{O}_2$ ) for 20 min and rinsed with copious amounts of water. *Caution: Piranha solution reacts violently with organic materials and should be handled carefully.* The cleaned quartz and silicon wafers were immersed in PDDA aqueous solution (1.0 mg/mL) for 20 min to obtain a cationic ammonium-terminated surface and were then ready for titanium phosphate multilayer deposition. The matrix titanium phosphate multilayer film was prepared by the layer-by-layer adsorption and reaction method reported previously<sup>19</sup> and described briefly as follows: The ammonium-terminated substrate was immersed in an aqueous solution of 10 mM  $\text{Ti}(\text{SO}_4)_2$  dissolved in 0.1 M  $\text{H}_2\text{SO}_4$

(16) Innocenzi, P.; Brusatin, G.; Martucci, A.; Urabe, K. *Thin Solid Films* **1996**, 279, 23.

(17) Akai, T.; Kadono, K.; Yamanaka, H.; Sakaguchi, T.; Miya, M.; Wakabayashi, H. *J. Ceram. Soc. Jpn.* **1993**, 101, 105.

(18) Bulinski, M.; Kuncser, V.; Plapcianu, C.; Krautwald, S.; Franke, H.; Rotaru, P.; Filoti, G. *J. Phys. D: Appl. Phys.* **2004**, 37, 2437.

(19) Wang, Q. F.; Zhong, L.; Sun, J. Q.; Shen, J. C. *Chem. Mater.* **2005**, 17, 3563.

(20) Clearfield, A. *Chem. Rev.* **1988**, 88, 125.

(21) Gao, G.; Rabenberg, L. K.; Nunn, C. M.; Mallouk, T. E. *Chem. Mater.* **1991**, 3, 149.

(22) Huang, X. Q.; Chen, Y. F. *Fine Specialty Chem.* **2001**, 18, 26.

for 5 min. Then, the substrate was transferred to the first PS solution (denoted as PS-1, pH 4.0) for a few seconds, after which it was immersed in the second PS solution (denoted as PS-2, pH 4.0) for 5 min. Finally, the substrate was rinsed with water and dried in a  $N_2$  stream. In this way, one layer of titanium phosphate was deposited on the substrate. Multilayer films of titanium phosphate could be prepared by alternately immersing the substrate into aqueous  $Ti(SO_4)_2$  and PS solutions.

**Silver Ion Incorporation and in Situ Synthesis of Silver Nanoparticles.** The procedure for silver ion exchange and in situ reduction to prepare silver nanoparticles in titanium phosphate films is illustrated in Scheme 1. Silver ions were incorporated into the as-prepared titanium phosphate film at room temperature and at 50 °C by immersing the film in 10 mM  $AgNO_3$  solution for 24 h. Then, the substrate was rinsed with deionized water for 1 min and dried in a  $N_2$  stream. The silver-ion-incorporated titanium phosphate film was immersed in freshly prepared 10 mM aqueous  $NaBH_4$  solution for 5 min, then rinsed with deionized water for 1 min, and finally dried in  $N_2$  stream to prepare silver nanoparticles.

**Measurements of Antibacterial Activity.** A 10-layer titanium phosphate film with silver ions adsorbed at 50 °C for 24 h was used to detect antibacterial activity. The substrate, both sides of which were coated with titanium phosphate film incorporated with silver ions, had a size of  $40 \times 10 \text{ mm}^2$ . A bacterial suspension of *Escherichia coli* (*E. coli*) was diluted to  $10^4$ – $10^5$  cfu/mL (cfu = colony forming units) in 5 mL Luria broth medium. With and without the addition of the silver-ion-exchanged titanium phosphate film, the suspension was cultivated at 37 °C for 18 h on a rotary shaker. After being properly diluted, *E. coli* was spread onto the agar plates from bacterial suspension. The agar plates were then inverted and incubated at 37 °C for 12 h. The number of colonies was counted to calculate the antibacterial activity.<sup>23</sup>

**Characterization.** UV–vis absorption spectra were recorded on a Shimadzu UV-3100 spectrophotometer. X-ray photoelectron spectroscopy (XPS) measurements were carried out on an ESCALAB Mark II (VG Company, U.K.) photoelectron spectrometer using a monochromatic Al K $\alpha$  X-ray source. Scanning electron microscopy (SEM) observations were carried out on a JSM-6700F scanning electron microscope with a primary electron energy of 3 kV. Transmission electron microscopy (TEM) observations were carried out on a JEM-2010 instrument operated at 200.0 kV.

## Results and Discussion

**Incorporation of Silver Ions into Titanium Phosphate Films Conducted at 50 °C.** Layered metal phosphates such as titanium phosphate and zirconium phosphate are known to exhibit rich intercalation chemistry because the protons in the layers can be exchanged with various kinds of cations.<sup>20,21</sup> This is also the case for the titanium phosphate films prepared by the layer-by-layer adsorption and reaction method. The as-prepared titanium phosphate films have an abundant amount of hydroxyl groups. At the same time, the porous structure of the titanium phosphate film facilitates the ion-exchange process with protons in hydroxyl groups. Figure 1a shows the UV–vis absorption spectra of an 8-layer titanium phosphate film before (solid line) and after (dashed line) immersion in an aqueous 10 mM  $AgNO_3$  solution at 50 °C for 3 h. The as-prepared film has an absorption peak near 230 nm. After immersion in  $AgNO_3$  solution, the

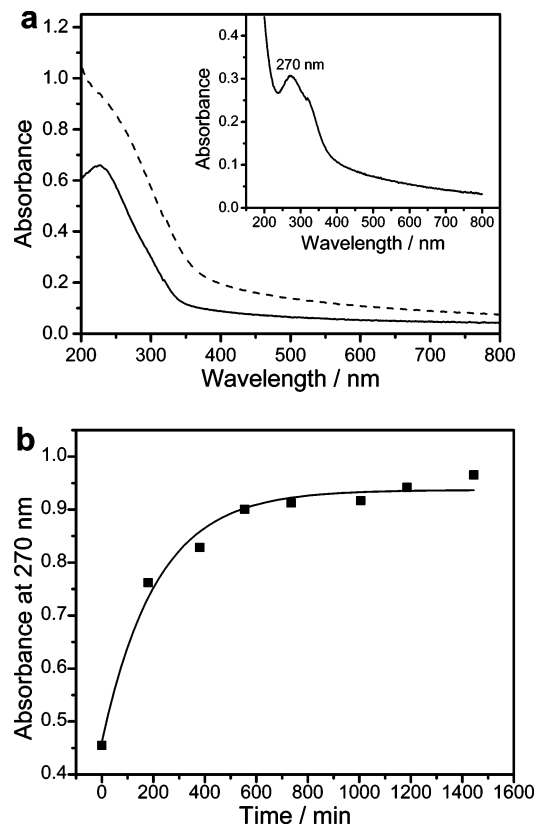


**Figure 1.** (a) UV–vis absorption spectra of an 8-layer titanium phosphate film before (solid line) and after (dashed line) immersion in an aqueous 10 mM  $AgNO_3$  solution at 50 °C for 3 h. Inset shows the UV–vis spectrum of silver ions after the solid line is subtracted from the dashed one. (b) Absorbance at 270 nm recorded as a function of time for the adsorption of silver ions into an 8-layer titanium phosphate film.

absorbance between 200 and 800 nm has increased, indicating the successful adsorption of silver ions. When the spectrum of the as-prepared titanium phosphate film was subtracted from that obtained after silver ion adsorption, a spectrum of the adsorbed silver ions was obtained, as shown in the inset of Figure 1a. The spectrum of the adsorbed silver ions shows an absorption peak at 270 nm. This peak at 270 nm can be used to monitor the adsorption dynamics of the silver ions. Silver ions were adsorbed at different time intervals on an 8-layer titanium phosphate film, and the absorbance at 270 nm was recorded. As shown in Figure 1b, the absorbance at 270 nm increased dramatically in the beginning and gradually reached a constant value after 10 h of adsorption, indicating a saturated adsorption of silver ions. An adsorption time of 24 h was used to ensure a maximum adsorption of silver ions into the titanium phosphate film and also to rationalize a comparison with the adsorption conducted at room temperature.

The incorporation of silver ions into the titanium phosphate films was further confirmed by XPS measurements. The XPS spectrum of an 8-layer titanium phosphate film deposited on a quartz wafer after 24 h of silver ion adsorption at 50 °C is shown in Figure 2a. No peak for Si 2p was detected because of the thick, full-coverage film obtained. Detailed analysis of the Ti, P, and O elemental composition of the film can be found in our previous report.<sup>19</sup> Briefly, Ti 2p<sub>1/2</sub> and Ti 2p<sub>3/2</sub> peaks are present at binding energies of 465.1

(23) Yan, J. H.; Zhai, F.; Ma, P. H.; Zhai, L.; Ying, H. Q. *Chin. J. Prev. Med.* **2002**, *36*, 114.

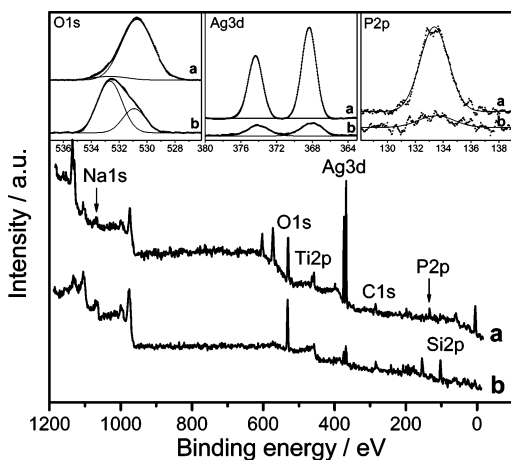


**Figure 2.** XPS spectra of an 8-layer titanium phosphate film after silver ion exchange for 24 h at 50 °C: (a) before and (b) after Ar<sup>+</sup> etching.

and 459.3 eV, respectively.<sup>19,24</sup> The P 2p signal peaks at 133.4 eV and consists of three peaks at 132.4, 133.4, and 134.7 eV, corresponding to binding energies for PO<sub>4</sub><sup>3-</sup>, HPO<sub>4</sub><sup>2-</sup>, and H<sub>2</sub>PO<sub>4</sub><sup>-</sup>, respectively.<sup>19,25</sup> An O 1s signal peaked at 530.8 eV was observed, which originated from O in P–O and P=O.<sup>26</sup> The ratio of P to Ti was 2.17, which is the same as that in the titanium phosphate film without silver ions incorporated.<sup>19</sup> Notably, Ag 3d<sub>5/2</sub> and Ag 3d<sub>3/2</sub> peaks at 368.4 and 374.4 eV, respectively, were observed, confirming the incorporation of silver ions into the titanium phosphate film.<sup>27</sup> The atomic ratio of P to Ag was determined to be 1:1.5 from their peak areas after correction of sensitivity factors. To further verify that the incorporated silver ions were dispersed homogeneously along the film normal direction of the whole titanium phosphate film and were not only on its surface, the titanium phosphate film after adsorption of silver ions in Figure 2a was etched with Ar<sup>+</sup> (3000 V, 40 μA) for 8 min and characterized again by XPS measurements. As shown in Figure 2b, a Si 2p peak at 103.6 eV was detected, indicating that the film became thinner after Ar<sup>+</sup> etching. The peaks of P 2p, Ag 3d, and Ti 2p in the etched film were still detectable, although their intensity decreased. The peak for O 1s shifted to 532.6 eV and can be deconvoluted into two peaks at 530.8 and 532.7 eV. The peak at 530.8 eV is the main assignment of O in P–O and P=O, whereas the other peak at 532.7 eV corresponds to O in Si–O.<sup>24</sup> The atomic ratio of P to Ag in the etched film was calculated to be 1:1.48. This result confirms that the incorporated silver ions were homogeneously dispersed along the film normal direction. The ion-exchange capacity for layered titanium phosphate was reported to be 7.76 mequiv/g, corresponding to an atomic ratio of P to Ag of 1:1.<sup>20</sup> The higher ion-exchange capacity of titanium phosphate film in our case is related to the porous structure of the film.

#### In Situ Reduction to Synthesize Silver Nanoparticles.

Figure 3a shows the UV–vis absorption spectra of a 9-layer

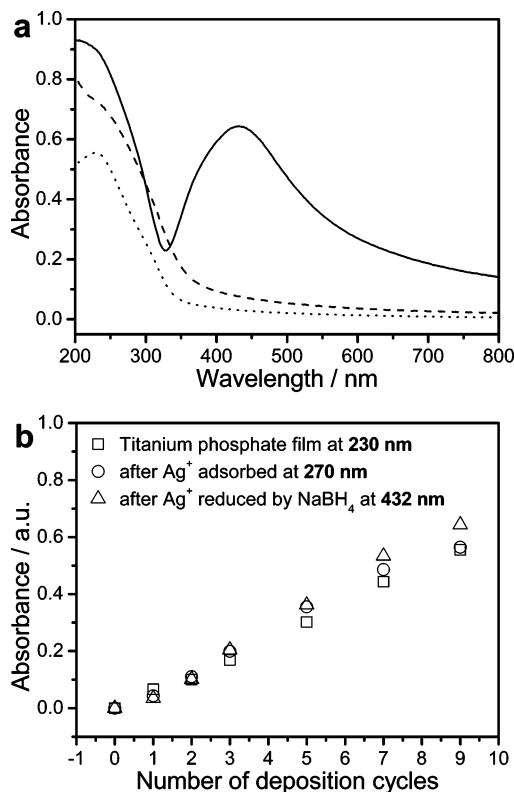


**Figure 3.** (a) UV–vis absorption spectra of a 9-layer titanium phosphate film (dotted curve) after the incorporation of silver ions at 50 °C for 24 h (dashed curve) and subsequent in situ reduction in NaBH<sub>4</sub> solution for 5 min (solid curve). (b) Maximum absorbance of the titanium phosphate film and the titanium phosphate film with silver ions and silver nanoparticles as a function of the number of titanium phosphate layers.

titanium phosphate film (dotted curves) after the incorporation of silver ions (dashed curves) and subsequent in situ reduction in NaBH<sub>4</sub> solution (solid curves). After the incorporation of silver ions into the titanium phosphate film, the absorbance between 200 and 800 nm increased, as observed in Figure 1a. After reduction in 10 mM aqueous NaBH<sub>4</sub> solution for 5 min, a peak at 432 nm was observed, which is the typical surface plasma resonance band of silver nanoparticles.<sup>28,29</sup> This result confirms the formation of silver nanoparticles in the film.

Titanium phosphate films with different numbers of layers were immersed in AgNO<sub>3</sub> solution for 24 h at 50 °C to incorporate silver ions and were then reduced in NaBH<sub>4</sub>. Their spectra were recorded for comparison. Figure 3b shows the maximum absorbance of titanium phosphate film and titanium phosphate film with silver ions and silver nanoparticles as a function of the number of titanium phosphate layers. The linear increase of the absorbance at 230 nm for titanium phosphate films indicates a satisfactory deposition process with almost equal amounts of titanium phosphate deposited in all of the layers.<sup>19</sup> At the same time, the linear increase of the absorbance at 270 nm after the incorporation of silver ions and at 432 nm after the formation of silver nanoparticles confirms that the amounts of silver ions and silver nanoparticles in each layer are almost equal. This result supports the XPS result that silver ions are incorporated

(24) Alfaya, A. A. S.; Gushikem, Y. *Chem. Mater.* **1998**, *10*, 909.

(25) Wang, J. Q.; Wu, W. H.; Feng, D. M. *Introduction to X-ray Photoelectron Spectroscopy*; Guofang Press: Beijing, 1992 (in Chinese).

(26) Tosatti, S.; Michel, R.; Textor, M.; Spencer, N. D. *Langmuir* **2002**, *18*, 3537.

(27) Jin, Y.; Dong, S. *J. Phys. Chem. B* **2003**, *107*, 12902.

(28) He, J. H.; Ichinose, I.; Kunitake, T.; Nakao, A. *Langmuir* **2002**, *18*, 10005.

(29) Ung, T.; Liz-Marzan, L. M.; Mulvaney, P. *Langmuir* **1998**, *14*, 3740.

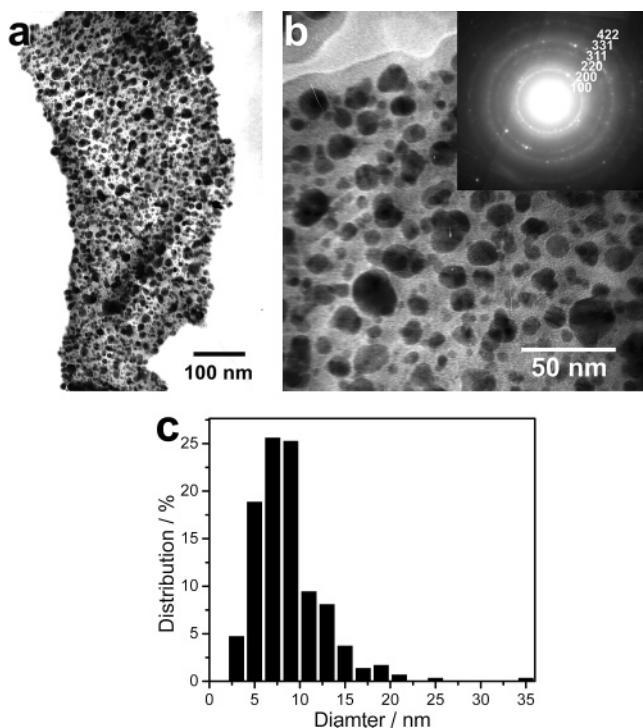
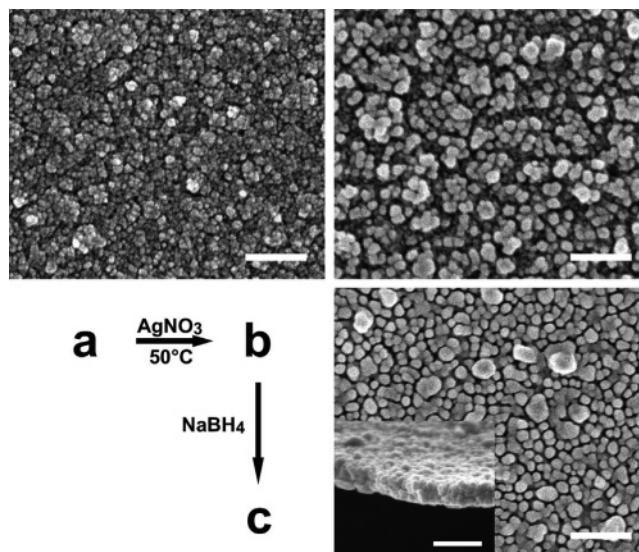


**Figure 4.** (a) TEM images of a piece of 6-layer titanium phosphate film after silver nanoparticle formation by ion exchange conducted at 50 °C. (b) Magnified image. Inset: SAED pattern. (c) Histogram of silver nanoparticles.

homogeneously along the film normal direction of the whole titanium phosphate matrix film.

A 6-layer titanium phosphate film containing silver nanoparticles prepared by silver ions adsorbed at 50 °C was scratched off from the quartz substrate in ethanol and transferred to a TEM grid for TEM observation. Figure 4a shows the TEM image of a whole piece of titanium phosphate film containing silver nanoparticles. Figure 4b shows a magnified image of the film. Silver nanoparticles can clearly be seen. The selected-area electron diffraction (SAED) pattern in the inset of Figure 4b shows clearly the (100), (200), (220), (311), (331), and (422) planes of the Ag nanoparticles. It is clear that the silver nanoparticles prepared in titanium phosphate film were crystallized. By sampling 300 silver nanoparticles, the histogram (shown in Figure 4c), mean diameter, and standard deviation were obtained. The mean diameter of the silver nanoparticles was calculated to be 8.6 nm, with a standard deviation of 3.9 nm.

The surface morphologies of the as-prepared 20-layer titanium phosphate film and the same film after silver ion adsorption at 50 °C for 24 h and formation of silver nanoparticles were investigated by SEM. As shown in Figure 5a, the surface of the as-prepared titanium phosphate film was uniform, comprising tiny particles with an average diameter of  $22.1 \pm 3.8$  nm. Large particles with a size of  $33.7 \pm 6.6$  nm and increased pores appear after ion adsorption at 50 °C for 24 h (Figure 5b). The large particles result from aggregation of the titanium phosphate film at elevated temperature. After the formation of silver particles, even larger aggregates appear, but the surface of the resultant film becomes smoother than that before reduction (Figure 5c). The inset in Figure 5c shows a cross-sectional SEM



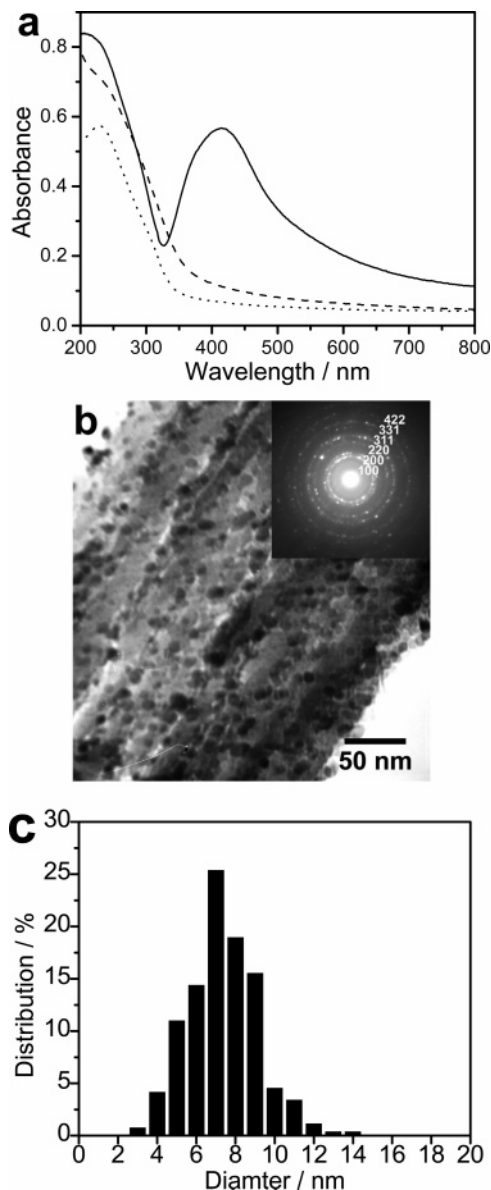
**Figure 5.** SEM images of a 20-layer titanium phosphate film: (a) as-prepared, (b) silver-ion-exchanged at 50 °C for 24 h, and (c) after the formation of silver nanoparticles. The scale bars correspond to 200 nm.

image of the film after the formation of silver nanoparticles, which has a constant thickness of 78 nm. The as-prepared 20-layer titanium phosphate has a thickness of ca. 72 nm, as one layer of titanium phosphate film has a thickness of  $3.6 \pm 0.5$  nm.<sup>19</sup> It is reasonable that the formation of silver nanoparticles leads to an increase of the film thickness.

#### Silver Ions Exchanged at Room Temperature and Subsequent Reduction to Prepare Silver Nanoparticles.

The incorporation of silver ions into titanium phosphate films is temperature-dependent, which will also have an influence on the silver nanoparticles synthesized in situ. At room temperature, saturated adsorption of silver ions takes 24 h, which is slower than that conducted at 50 °C. For comparison, a 24-h adsorption at room temperature was also used to prepare silver-ion-exchanged titanium phosphate films. UV-vis absorption spectra of titanium phosphate films with different numbers of layers after adsorption of silver ions show that silver ions adsorbed at room temperature are dispersed homogeneously along the normal direction of the titanium phosphate films. UV-vis spectra of a 9-layer titanium phosphate film before and after the formation of silver nanoparticles are shown in Figure 6a. Silver nanoparticles prepared by ion exchange conducted at room temperature have a surface plasma peak at 420 nm, which is blue shifted when compared to those synthesized by adsorption at 50 °C, indicating that silver nanoparticles with a smaller size were obtained at lower adsorption temperature. The TEM image in Figure 6b and the size distribution in Figure 6c show that silver nanoparticles with a particle size of  $7.4 \pm 1.8$  nm were synthesized. SAED results in the inset of Figure 6b reveal that well-crystallized silver nanoparticles were obtained.

**Antibacterial Activity of Ag<sup>+</sup>-Incorporated Titanium Phosphate Film.** Silver metal and silver salts are the most widely used antimicrobial agents for wound care because of their ability to kill a broad spectrum of infectious bacteria.<sup>10</sup> Silver is usually incorporated into a solid support to realize a sustained release of silver ions and a long-term antibacterial activity. Recent research shows that silver can be easily



**Figure 6.** (a) UV-vis absorption spectra of a 9-layer titanium phosphate film (dotted curves) after the incorporation of silver ions at room temperature for 24 h (dashed curves) and subsequent in situ reduction in  $\text{NaBH}_4$  solution for 5 min (solid curves). (b) TEM image of an 8-layer titanium phosphate film after silver nanoparticle formation by ion exchange conducted at room temperature. Inset: SAED pattern. (c) Histogram of silver nanoparticles.

incorporated into polyelectrolyte films. Polyelectrolyte films containing silver species are a type of promising antibacterial coating because these coatings can, in principle, be prepared on substrates with any morphologies and the thickness of the coatings, content of silver, and sustained release of silver are easily controlled.<sup>6,9,10</sup> Compared to polyelectrolyte films, inorganic films such as titanium phosphate show higher chemical and mechanical durabilities. The high durability of the matrix titanium phosphate films is expected to be helpful in widening the application window of silver-ion-exchanged titanium phosphate films. Previous studies have shown that the ionic form of silver is responsible for antimicrobial action.<sup>10,30</sup> Therefore, titanium phosphate films incorporated with silver ions were further examined as

(30) Simonetti, N.; Simonetti, G.; Bougnol, F.; Scalzo, M. *Appl. Environ. Microbiol.* **1992**, *58*, 3834.

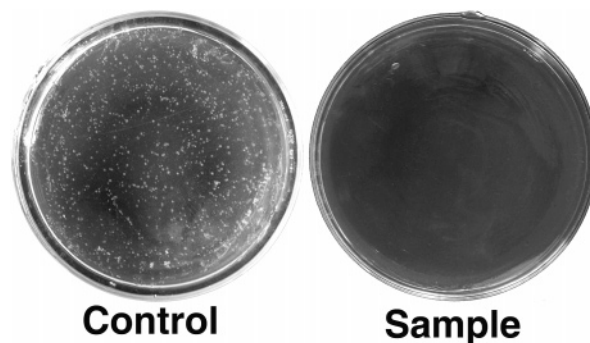


**Figure 7.** Photographs of colonies of *E. coli* incubated on agar plates obtained from cultivated suspensions with (control) and without (sample) silver-ion-exchanged titanium phosphate film.

antibacterial coatings. A 10-layer titanium phosphate film after 24 h of adsorption of silver ions at 50 °C was used, and its inhibition of *E. coli* growth was investigated. The antibacterial activity of the silver-ion-exchanged titanium phosphate film was tested following the procedure outlined in the Experimental Section. In a control experiment, the nearly transparent *E. coli* suspension without a silver-ion-exchanged titanium phosphate film became turbid as a result of the propagation of *E. coli*. After being shaken for 18 h at 37 °C, the bacterial suspension containing a silver-ion-exchanged titanium phosphate film remained nearly transparent with a yellowy color. This result shows that the silver-ion-exchanged titanium phosphate film, even with a thickness of  $\sim 39$  nm, has the ability to inhibit the growth of *E. coli*. Furthermore, 0.1 mL aliquots of a suspension after 18 h of shaking with and without antibacterial substrate were diluted  $1 \times 10^5$  times. Then, 0.1 mL of each diluted suspension was spread onto agar plates and incubated separately at 37 °C for 12 h. The number of surviving *E. coli* was estimated by counting the exact number of colonies shown in Figure 7. The antibacterial rate was calculated using eq 1<sup>23</sup>

$$\text{antibacterial rate (\%)} = \frac{N_{\text{control}} - N_{\text{sample}}}{N_{\text{control}}} \times 100\% \quad (1)$$

where  $N_{\text{control}}$  and  $N_{\text{sample}}$  correspond to the numbers of colonies calculated per milliliter from the control and from the experiment with  $\text{Ag}^+$ -incorporated titanium phosphate film, respectively. An antibacterial rate greater than 99.9% was obtained, indicating that an effective antibacterial coating of silver-ion-exchanged titanium phosphate film had been prepared. It should be mentioned that silver ions interact strongly with the phosphate group of the titanium phosphate matrix film in our case. This might be helpful to realize a sustained release of silver ions. A detailed investigation is still underway.

## Conclusions

In the present study, we show that silver ions can be incorporated into titanium phosphate ultrathin films by a simple ion-exchange process. By in situ reduction, silver-nanoparticle-loaded titanium phosphate films were successfully prepared. The ion-exchanged titanium phosphate films

are effective in prohibiting the growth of *Escherichia coli* and, therefore, can be used as a promising kind of antibacterial coating. Considering the high mechanical and chemical stabilities of the matrix titanium phosphate film used, the silver-doped titanium phosphate film can be used in a wide range as catalyst and antibacterial coatings. The high ion-exchange capacity of the titanium phosphate film as exemplified by silver ions and its easy deposition on substrates with complicated morphologies will make titanium phosphate

films excellent candidates for removing heavy metals from water.

**Acknowledgment.** This work was supported by National Natural Science Foundation of China (NSFC Grant 20304004), Foundation for the Author of National Excellent Doctoral Dissertation of P. R. China (FANEDD Grant 200323), and Program for Changjiang Scholars and Innovative Research Team in University (PCSIRT Grant IRT0422).

CM052654I